IPP-Report

Max-Planck-Institut für Plasmaphysik

B. Nold E. Holzhauer H.W. Müller L. Kammerloher
ASDEX Upgrade Team

Electronic issues of Langmuir probe measurements on the midplane manipulator of ASDEX Upgrade

IPP 10/43
Dezember, 2012

Electronic issues of Langmuir probe measurements on the midplane manipulator of ASDEX Upgrade

B Nold*and E Holzhauer
Institut für Plasmaforschung
Universität Stuttgart, 70569 Stuttgart, Germany

H W Müller†, L Kammerloher and the ASDEX Upgrade Team
Max-Planck-Institut für Plasmaphysik
EURATOM Association, Garching, Germany

Abstract

A detailed knowledge of the Langmuir-probe electronics is crucial to avoid measurement errors. Probe signals from the midplane manipulator of the ASDEX Upgrade tokamak have been affected by electronic issues. The related perturbations could exceed the plasma fluctuation amplitudes significantly and can not be removed by postprocessing from the digitized data. The electronic probe system suffered from cross-talk between different measurement channels, magnetic pick-up, resonant amplifier oscillations and a limited frequency transmission. These effects have been explained, reproduced and suppressed in SPICE simulations, laboratory experiments and finally on the ASDEX Upgrade probe system. A change of the ground connection in 2010 minimized pick-up and reduced the cross-talk by three orders of magnitude. New low-pass filters suppress aliasing effects since March 2011. Furthermore, the transmission range of floating potential fluctuations is increased since that time by preamplification of the signals. The present work explains in detail the investigation and adaptation of the Langmuir-probe system to enable the interpretation of experimental probe data from different experimental campaigns and to facilitate the setup of reliable probe measurements at ASDEX Upgrade and similar devices.

*nold@ipf.uni-stuttgart.de
†hwm@ipp.mpg.de

1 Introduction

Energy and particle losses in the edge of magnetically confined plasmas are dominated by turbulent transport [1]. A significant fraction of the radial transport in low-confinement (L-mode) [2] and in between edge localized modes (ELMs) in high-confinement (H-mode) discharges is related to blobs [3]. These filaments have sizes and velocities perpendicular to the magnetic field lines of about 1 cm and 1 km/s, respectively [4]. Correspondingly, a sub-cm spatial and 10 μs temporal resolution is required to study their dynamics.

Langmuir probes can provide spatially ($1 - 2$ mm) and temporally (0.5 μs) well defined measurements of ion-saturation current (I_{sat}) and floating potential (Φ_{fl}). However, great care has to be taken to assure reliable fluctuation measurements of the probe system. This work presents possible perturbations of Langmuir-probe signals, points out the underlying electronic reasons and possible solutions. It is intended to help judging the quality of old and future Langmuir-probe data and similar experiments. Furthermore, it is a call for careful experimentation and data analysis. It might help to identify and avoid electronic issues in future work at ASDEX Upgrade and similar devices.

During the last years, various Langmuir probe heads have been installed on the mid-plane manipulator of ASDEX Upgrade [5]. The same wiring and data acquisition system has been used in most of these experiments. The data presented here was measured with the multi-pin probe head [4] during experimental campaigns in October 2009 and April and November 2008. Measurements with other probe heads during this period (and possibly before) are expected to behave in the same way.

The following section describes the Langmuir Hotlink system, as it was commonly used at the midplane manipulator of ASDEX Upgrade before the experimental campaign in autumn 2010. Measurements with this system led to the perturbations in the probe data, as shown in Sec. 3. The reasons for these perturbations were inductive coupling between different measurement channels (Sec. 4), resonant oscillations of the anti-aliasing filters (Sec. 5) and low-pass filtering of the transmission lines (Sec. 6). Solutions to suppress these effects are pointed out in the following and have been implemented at ASDEX Upgrade during the experimental campaign 2010/2011. A short summary and conclusions are given in Section 7.

2 Probe setup before 2010

Before the experimental campaign in 2010, Langmuir probes on the midplane manipulator of ASDEX Upgrade have been connected to the data acquisition system as shown in Figure 1. The Langmuir probe tips in the vacuum vessel were connected with 15 - 25 m long coaxial cables to the data acquisition system. The outer conductor of these cables was interrupted in a grounded metal box at the manipulator exit about 10 m behind the probe tips. The ends of this shielding were not terminated, i.e. the magnetic inductance of currents along

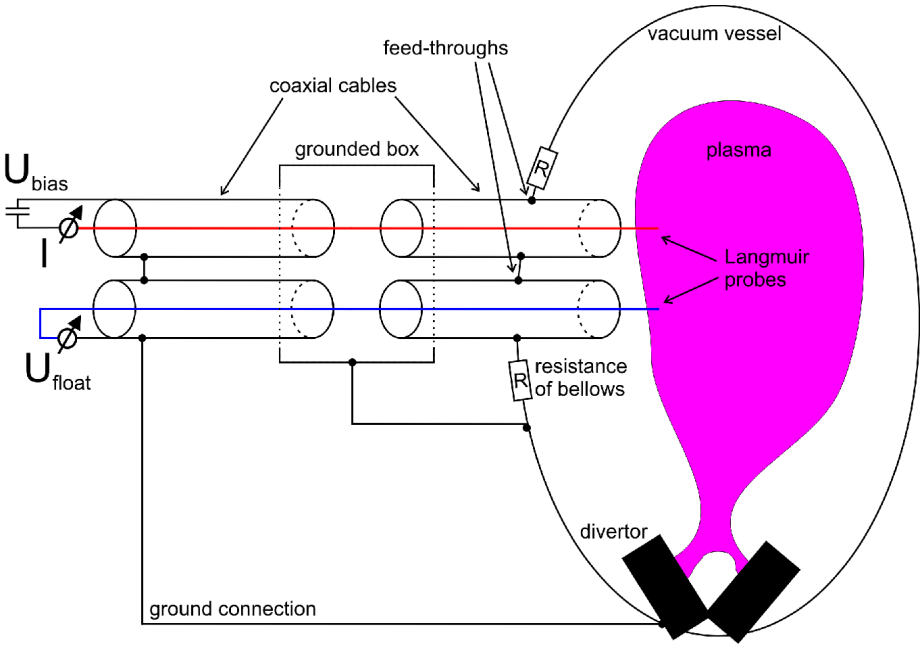

Figure 1: Sketch of the former Langmuir probe system at the midplane manipulator. The measurement occurs at the end of two coaxial cables connected in series with interrupted shielding. Both parts are grounded separately either at the divertor or directly at the manipulator vacuum feed-throughs which are connected with the vessel via the resistance of the movable bellows.

the inner conductor was not compensated by currents along the shielding. The shielding was only electrostatic. The front part of the shieldings were connected electrically with the midplane manipulator at the vacuum feed-throughs about 10 cm behind the probe tips. The manipulator is connected via the bellows to the vacuum vessel and divertor targets. The bellows are have a finite resistance that might cause a potential difference between divertor and manipulator. The bellows are represented by the resistances (R) in Fig. 1. The other part of the shielding was not terminated in the metal box and at the other end connected to the data acquisition system. This side was (at least since 2008) grounded separately in the divertor.

Another movable probe system at ASDEX Upgrade is the so-called filament probe [6]. It is mounted at another position in the torus and consists of Langmuir and magnetic probes. As shown in Figure 2, these probes are connected to the data acquisition with continuously shielded coaxial cables. The whole measurement system is floating except for one ground connection at the vacuum feed-through. These feed-throughs are in good electrical contact with the vacuum vessel because there are no bellows in between.

Current and potential of all probes are measured with so-called Langmuir-

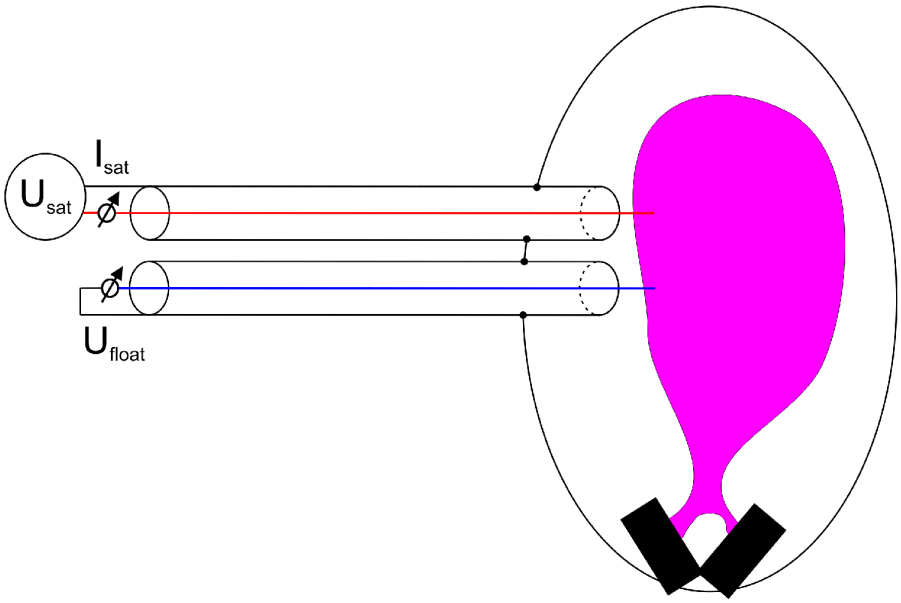

Figure 2: Sketch of the present filament probe setup. The measurement occurs at the end of two coaxial cables with a single connection point to the vessel. The reference potential is directly connected from the vacuum feed-through over the outer conductor of the coaxial cable to the diagnostic.

Hotlink devices [7]. They contain measurement resistors, signal amplification, anti-aliasing filters and the analog to digital conversion with a rate of 2 MHz. The Langmuir-Hotlink devices are floating to enable a free choice of the reference potential without generation of ground loops. The digitized signals of 8 Langmuir-Hotlink systems are stored under the so-called MHC diagnostics. Further 8 Langmuir-Hotlink systems are combined under the so-called MHG diagnostics. The length of the coaxial cables from the metal box at the manipulator exit to the Langmuir-Hotlink devices of MHC and MHG are about 5 and $10 - 15$ m, respectively. The Langmuir-Hotlink devices can be adjusted to measure probe currents of ± 0.1, ± 1.0 or ± 10 A with a 14 bit resolution, appropriate to the plasma conditions. Temporally varying bias voltages cause currents to the coaxial cables, even in absence of plasma at the Langmuir probe tips. These currents are due to the capacitance of the relatively long connection cables between probe tip and measurement. The corresponding signals can be suppressed for a specific setup and bias voltage in the measurement by adjusting two compensation circuits in the Langmuir-Hotlink devices. The MHC channels can be switched to measure floating potentials with a high input resistance of 1.1 MΩ. A detailed up-to-date documentation of the ASDEX Upgrade Langmuir probe system and the status of the Langmuir-Hotlink systems can be found in [8] and [9], respectively. The examples in the next section show how probe data pertur-

bations can look like. The following sections address the different reasons and suggest solutions to avoid such perturbations in Langmuir probe measurements.

3 Probe perturbations before 2010

This section deals with Langmuir probe perturbations that have been identified in measurements using the midplane manipulator of ASDEX Upgrade during the experimental campaigns of the years 2008 and 2009. Figure 3 shows time slices from the floating potential measurement of a Langmuir probe (Φ_{fl}, top), as well as the current (I, middle) and applied voltage (U, bottom) of an other probe during an L-mode phase. The sweeping frequency of 10 kHz was chosen to obtain a good temporal resolution of the electron temperature without approaching the limits of this technique [10]. The minimum bias voltage of $-180\,\mathrm{V}$ was chosen to assure ion current saturation even for negative floating potentials and high temperatures. The bias voltage was swept symmetrically into ion and electron branch, because the IPP temperature fitting routine considers both, ion and electron saturation branch [11]. The shown signals correspond from left to right to measurements before plasma ignition, in the SOL and twice just a few millimeters outside the separatrix. Both probes are mounted on the midplane manipulator and separated poloidally by 8 mm. Strong fluctuations of the floating potential (top) are observed periodically in all four time slices. The fluctuations on the left can not be related to plasma fluctuations, because the plasma was not yet ignited at that time. The periodicity of the strong floating potential fluctuations seems to coincide with fast current variations on the sweeping probe (middle). This indicates a cross-talk between different measurement channels, which might occur at the probe tips, in the connecting cables or between Langmuir-Hotlink systems. The amplitudes of these floating potential perturbations exceed the background fluctuations significantly at all radial positions and can therefore not be neglected in the data analysis.

The left column in Fig. 3 shows the behavior without plasma. Currents (I) of a few mA should charge the cable capacitance (C) corresponding to the applied voltage (U) according to $I = C\,\mathrm{d}U/\mathrm{d}t$. Current peaks are observed at the maxima of the applied voltage, when $\mathrm{d}U/\mathrm{d}t$ quickly changes sign. This is related to the self-inductance of the cables. The actually measured signal is modified by the compensation of rectangular and spike currents within the Langmuir-Hotlink system. By further adjustment, the signal in absence of plasma might even have been reduced to zero. However, the compensation modifies only the measured signal. It does not affect currents flowing in the cables between power supply and probe tip. The current compensation within the Langmuir-Hotlink devices should therefore not be able to minimize the observed cross-talk between different measurement channels. The two right columns of Fig. 3 show probe measurements of the midplanemanipulator close to the separatrix. Electron currents of more than 6 A are drawn over the swept probe tip due to the high positive bias voltages. The so-called L5 battery packages can maintain such high currents only for a limited time before their voltage breaks down (bottom

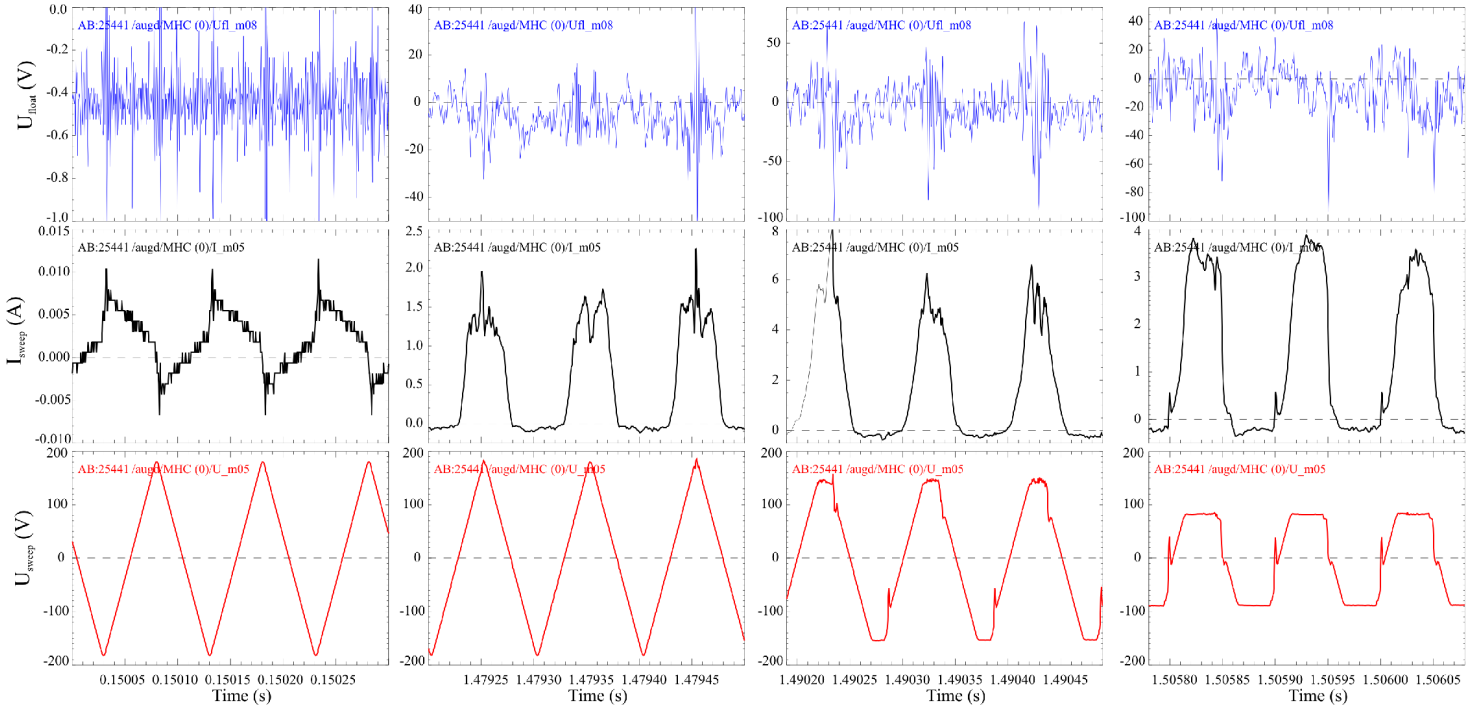

Figure 3: Floating potential (top) compared to current (middle) and bias voltage (bottom) of a sweeping Langmuir probe at different times (radial positions) during the first L-mode phase of discharge #25441. Large floating potential pulses with amplitudes of up to 150 V coincide with fast current variations.

right). The fast current changes provoke significant potential perturbations on floating probes, even when the bias voltage has dropped by more than 50 %.

Figure 4 compares floating potential measurements from midplane manipulator and filament probe with the current characteristics of a swept Langmuir probe on the manipulator. All floating probes on the midplane manipulator show perturbations related to high electron currents through the swept Langmuir probe. The measurement of the filament probe at another toroidal position is unaffected. All signals have been acquired with the Langmuir-Hotlink systems of the MHC diagnostics. All signals should show perturbations, if the cross-talk would occur inside the Langmuir-Hotlink devices. The unaffected signal of the filament probe indicates therefore, that the cross-talk between measurement channels occurs at the probe tips or in the connecting cables, but not between the Langmuir-Hotlink systems. The highest perturbation amplitudes are observed on probe number 8, while the probe tips number 9 and 10 are located closer to the sweeping probe tip number 5. Probe interactions in the probe head or through local plasma modification would certainly act strongest between neighboring probes, which is not observed here. This indicates that the observed coupling is not due to plasma modifications or other local electro-magnetic effects at the probe head. The cross-talk between different measurement channels is therefore supposed to be related to the connecting cables between the Langmuir-Hotlink systems and the probe head on the midplane manipulator.

Figure 5 shows some more time slices of Langmuir probe measurements on the midplane manipulator of ASDEX Upgrade. The signals are from top to bottom: (i) floating potential of probe number 8 (MHC), (ii) ion-saturation current of probes number 3 (MHC) and 6 (MHG), (iii) zoom into ion branch of current characteristic at probe number 5 (MHC) and (iv) ion-saturation current of probes number 1 (MHG) and 12 (MHG). Periodic perturbations are observed in floating potential and ion-saturation current measurements, when high electron currents are drawn through the sweeping probe (here out of range). The strongest ion-saturation current perturbations are observed on probe number 6, which hast the largest distance to the sweeping probe (19 mm) and is recorded with a Langmuir-Hotlink system of the MHG diagnostics. This confirms the previously made conclusions, that the cross-talk is caused by the cables between probe head and Langmuir-Hotlink devices. Strong perturbations have been observed in potential and current measurements on the midplane manipulator of ASDEX Upgrade during the experimental campaign in 2009.

Perturbations have also been observed in Langmuir probe signals from the year 2008, as shown in the following. Figure 6 shows a zoom into the floating potential measurements (top) from April 2008. All potentials show a sudden perturbation followed by a short oscillation at 1 MHz, although there is no plasma present at the probe. The potential perturbations occur always when the bias voltage of ion-saturation current measurements (middle) is switched on or off. The bias voltage is interrupted regularly to extinct possible arcs between probe head and tips. In absence of plasma, this leads to short current pulses loading the cable capacitance as shown in the bottom of the figure. The

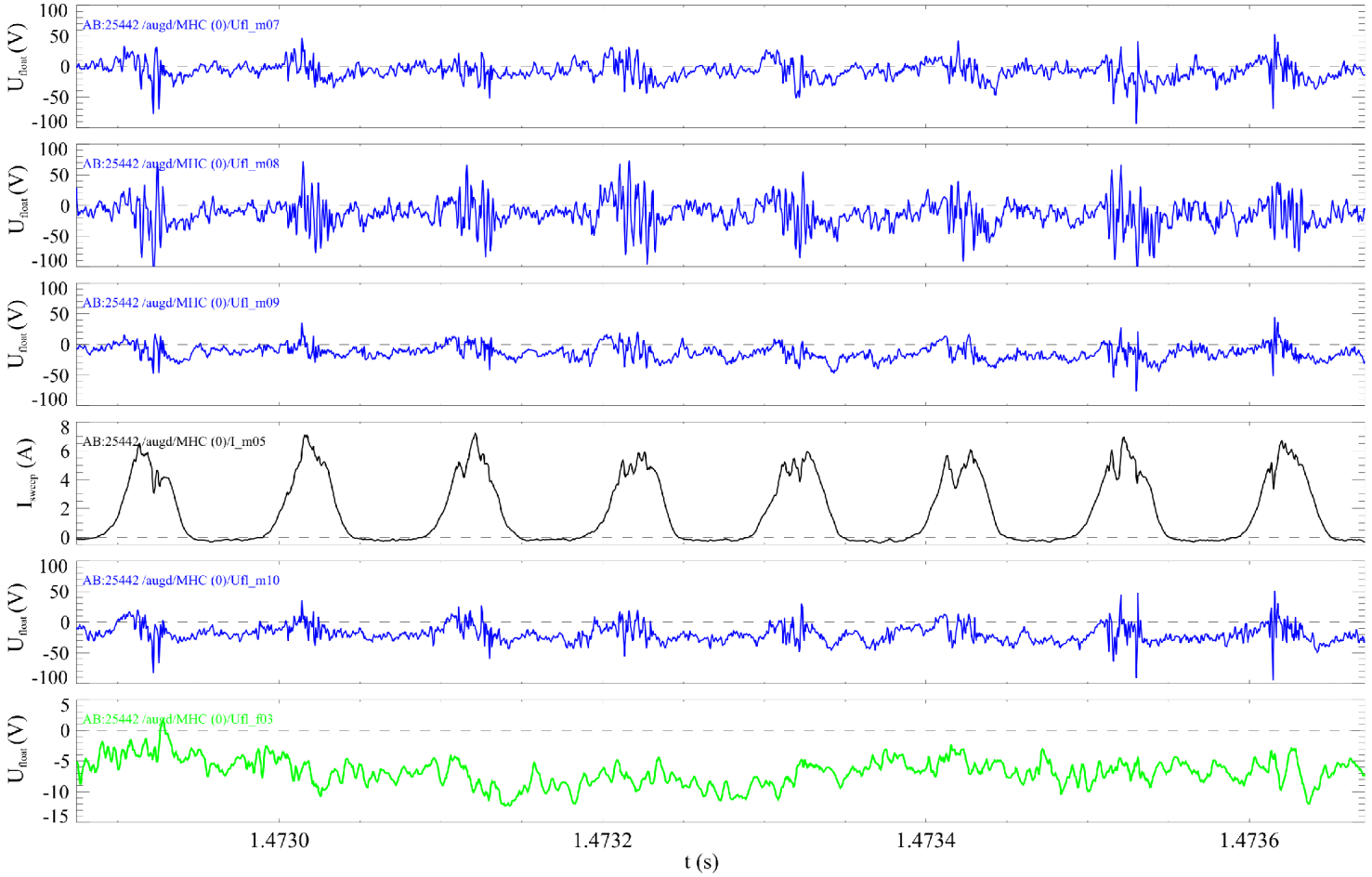

Figure 4: Floating potentials and current drawn by the sweeping Langmuir probe. Probes are ordered in the vessel from top to bottom as shown here except the floating potential from the filament probe (bottom), which was measured at another toroidal position.

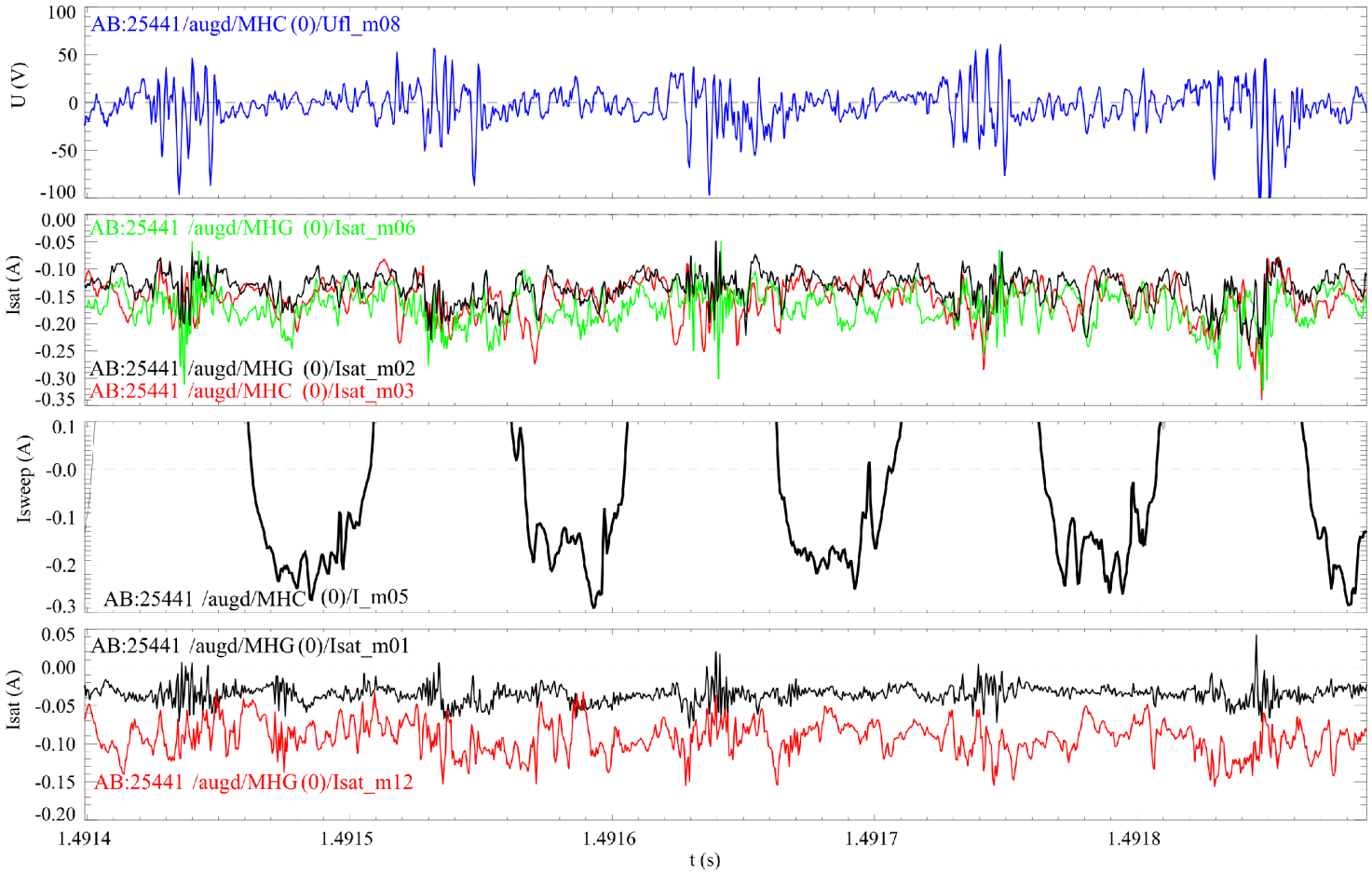

Figure 5: Time traces of measured floating potential (top) and different probe currents: top level ion saturation currents I_{sat} (second plot), current of sweeping probe (third plot) and I_{sat} of radially retracted probes (bottom).

coincidence of current pulses and floating potential perturbation indicates again a current dependent cross-talk between measurement channels. The clearly visible oscillation with the Nyquist-frequency in the digitized data indicates that the anti-aliasing filter of the Langmuir-Hotlink devices did not work properly. This last topic will be addressed in Section 5. Similar cross-talk has also been observed in probe data from the experimental campaign in November 2008, as shown in Fig. 7.

Figure 8 shows floating potentials (top), ion-saturation currents (middle) and the current of a swept Langmuir probe (bottom) in presence of plasma during the experimental campaign in April 2008. The floating potentials oscillate for about $20\,\mu$s at a frequency of 400 kHz. The amplitude of this oscillation is two orders of magnitude larger than the turbulent fluctuations before and after this event. A similar oscillation is also observed in one of the ion-saturation current measurements. The reason for these oscillations might be triggered by the fast drop of the electron current in the sweeping probe. A similar coincidence of changing current and floating potential is marked earlier in the same figure. It is quite difficult to distinguish local fluctuations of the plasma parameters at the probe tip and cross-talk effects from other probes. This fact is further illustrated by figure 9 for the experimental campaign from November 2008. Here a high density event is observed in the swept probe and ion-saturation current signals, but followed by a 400 kHz oscillation in one or two of the saturation current measurements. Most of the floating potential measurements show the same oscillation, but during the entire time slice.

The results of this section can be summarized as follows:

- Langmuir probe signals contained non-plasma perturbations.
- Perturbations have been found in the experimental campaigns from 2009, as well as from April and November 2008. The perturbations are therefore not likely to be caused by an unique mistake, but rather due to a systematic problem of the probe setup.
- The perturbations consist of cross-talk between measurement channels and large amplitude oscillations with frequencies up to the Nyquist-frequency.
- The cross-talk is connected to the cables of the midplane manipulator and therefore independent of probe head and the Langmuir-Hotlink device in use. Similar perturbations are therefore also expected for other probe heads during these campaigns.
- Perturbations are sometimes difficult to distinguish from turbulent fluctuations. However, their amplitudes can exceed turbulent fluctuations significantly and can therefore not be neglected.

The cross-talk of measurement channels is further characterized and explained in the following section. The aliasing issue and transmission of high frequency signals are addressed in Sections 5 and 6.

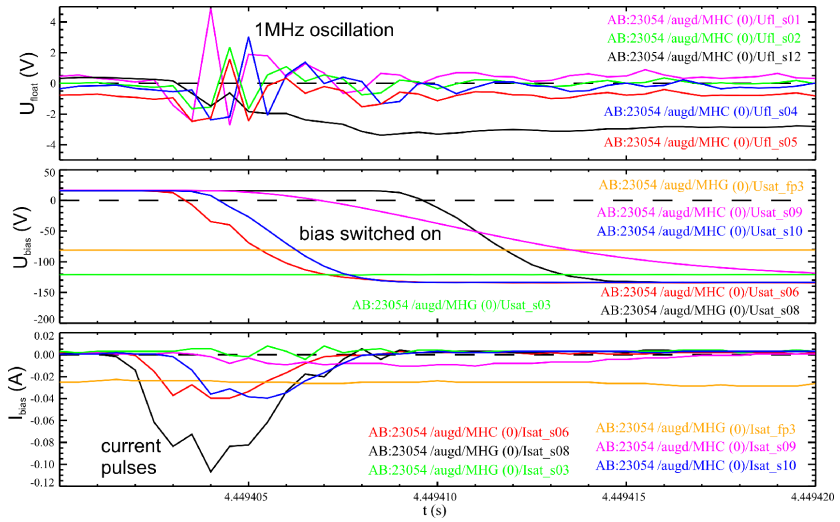

Figure 6: Probe signals from April 2008 without plasma. All floating potentials (top) show significant perturbations at the Nyquist-frequency of 1 MHz, when the negative bias is applied (middle) to measure the ion-saturation current (bottom). In absence of plasma only a current pulse is flowing to charge the cable capacitance.

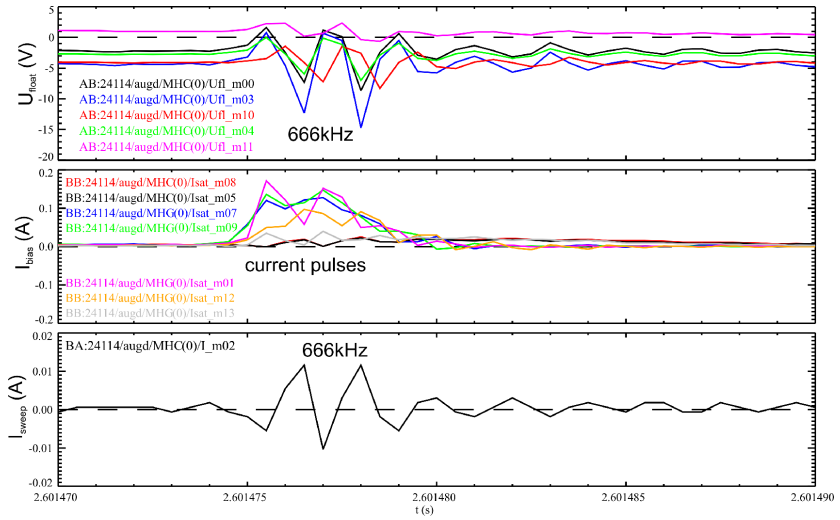

Figure 7: Probe signals from November 2008 without plasma. Floating potentials (top) and the current of the swept probe (bottom) start to oscillate at 666 kHz when the cable capacitances of the ion-saturation current probes are discharged (middle).

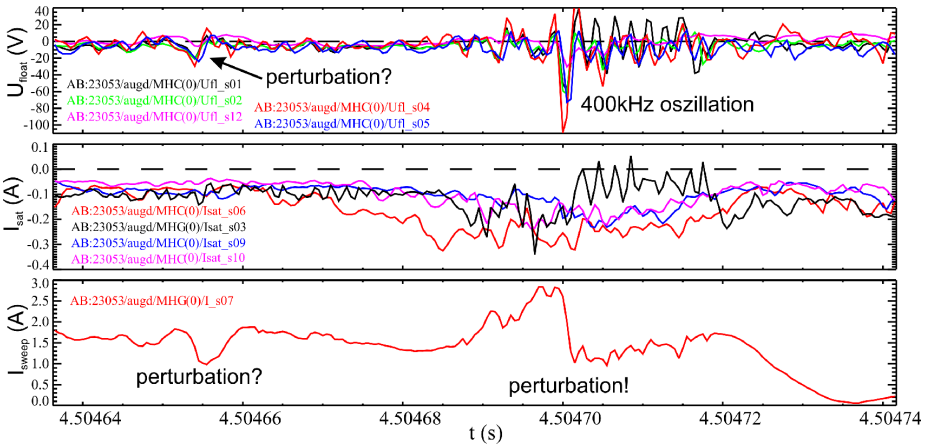

Figure 8: Probe signals from April 2008 with plasma. All floating potentials (top) and one ion-saturation current start to oscillate at 400 kHz after an abrupt current and potential drop on the sweeping probe (below). Not clear is the origin of an earlier floating potential modification.

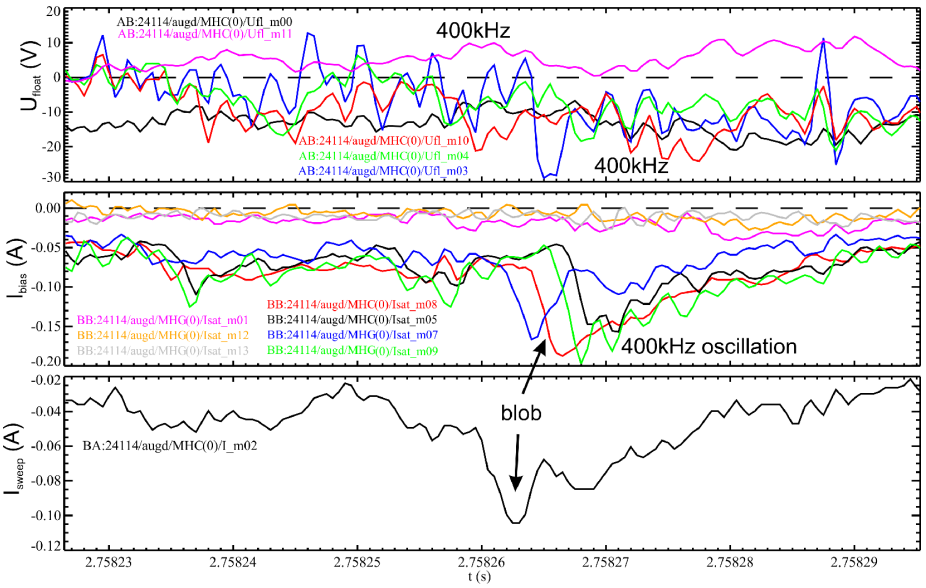

Figure 9: Probe signals from November 2008 with plasma. Top level floating potential probe signals fluctuate significantly at 400 kHz (top). No consistent phase shift is observed between probes. A blob propagates poloidally downward from the swept probe (bottom) and across the top level ion-saturation current probes (center). A physically unexpected 400 kHz oscillation is observed in two current signals during the density decay.

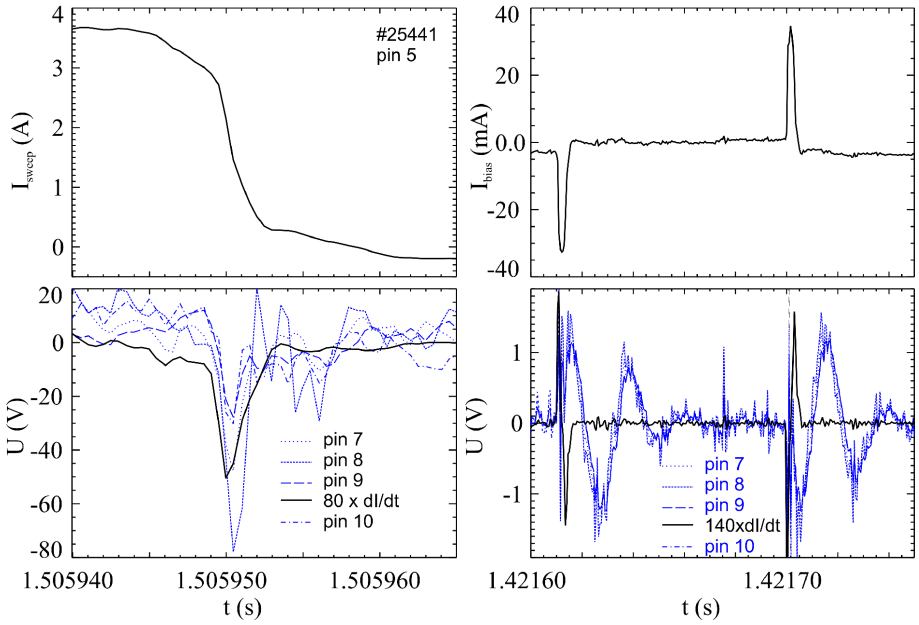

Figure 10: Top: Currents flowing through probes on the midplane manipulator. Left: The potential of the swept Langmuir probe in the plasma changed from positive to negative. Right: Current pulses discharged and charged the cable capacity of a probe outside the plasma, when the bias voltage is switched off and on. Bottom: Temporal derivation of these currents (black solid lines) compared with the floating potential on neighboring probe channels.

4 Inductive coupling

It has been shown in the previous section, that varying probe currents can lead to cross-talk with other probe measurements. This relation points to an inductive coupling between different cables, that was further investigated and finally reduced, as described in this section.

4.1 Experimental evidence

Figure 10 (left) shows a zoom into the temporal evolution of a cross-talk event between different Langmuir probe channels on the midplane manipulator of ASDEX Upgrade. The upper graph shows the fast decay from 4 A electron current to 0.2 A ion current drawn through a sweeping probe. The temporal derivative of the current reaches a maximum value of $\mathrm{d}I/\mathrm{d}t = -1.3\,\mathrm{MA/s}$. The lower graph compares the shape of an induced voltage $U_{\mathrm{exp}} = L_{\mathrm{exp}} \times \mathrm{d}I/\mathrm{d}t$ (solid line) with the four floating potential measurements on the mid-plane manipulator. The experimental coupling inductance $L_{\mathrm{exp}} = 80\,\mu\mathrm{H}$ was chosen

to fit U_{exp} to the range of floating potential perturbations. All four potential measurements show a negative peak with amplitudes between 40 and 80 V when $\mathrm{d}I/\mathrm{d}t$ reaches its maximum. The simultaneous variation of all floating potential measurements with the current change through the sweeping probe supports the model of inductive coupling. L_{exp} was found to vary between probes by a factor of two and between different probe positions in the plasma by a factor of three. The variation between probes might be due to the varying cable positions of different channels in the torus hall. The variation of L_{exp} with the probe position might be due to the corresponding cable motion and changing plasma parameters at the probe tips. The success of digital signal correction seems limited because several source currents (I_{sweep} and I_{sat}) need to be considered with each having a radially and plasma dependent coupling inductance. It is thus impossible to reconstruct the electrostatic fluctuations from the perturbed potential measurements.

Figure 10 (right) shows damped oscillations in the floating potential (bottom) that have been observed when the Langmuir probes were far away from the plasma. The oscillation seems to be inductively excited by the current pulses shown in the top. These pulses are observed when the bias voltage of ion-saturation current measurements is switched off periodically to interrupt possible arcs between probe head and probe. The solid line in Fig. 10 (bottom, right) shows the temporal derivation of the current pulses (top) multiplied with a coupling inductance of 140 μH. These 5 μs perturbations trigger damped oscillations of all floating potentials. This oscillation can be described by an equivalent RLC-circuit $U(t) = U_0 \ \cos(\omega t + \phi) \ \exp(-\alpha t)$ with the initial excitation U_0, the oscillation frequency $\omega = \sqrt{1/LC - R^2/4L^2}$ and the damping coefficient $\alpha = R/2L$. The latter two have been determined graphically from the measurement as $\omega \approx 300\,\mathrm{kHz}$ and $\alpha = 7.5 \times 10^4\,\mathrm{s}^{-1}$. Capacitance and self-inductance of a 20 m long coaxial cable are $C_{\mathrm{theo}} \approx 2\,\mathrm{nF}$ and $L_{\mathrm{theo}} \approx 1\,\mu\mathrm{H}$ [12], respectively. The resistance of the equivalent RLC-circuit can be deduced from these theoretical values and the measured oscillation frequency or damping coefficient to be $R(\omega) = 45\,\Omega$ or $R(\alpha) = 0.15\,\Omega$, respectively. The input resistance of the Langmuir-Hotlink device with 1.1 MΩ is much bigger. This resistance can not be part of the oscillation, because otherwise unrealistic inductances and capacities in the H and pF range would be necessary. The differential plasma impedance between probe and vacuum vessel can be in the range of 50 Ω. However, in the present case the probe is not in contact with the plasma. The observed oscillation is most probably damped by the resistance of the manipulator ballow, which was measured to be about 1.5 Ω. The observed oscillation would consequently be an oscillation between the two parts of the shield in Fig. 1 with a system inductance of 10 μH and capacitance of 1 μF. These values are realistic, although much bigger than what is expected for a continuous coaxial cable as shown in Fig. 2. The observations might be explained by high inductance due to the interrupted outer conductor. The following theoretical considerations support this model.

4.2 Theoretical evidence

This section presents a physics picture that can explain the cross-talk and will be verified experimentally later. According to Ampere's law, a current (j) provokes a circular magnetic inductance ($\mathbf{B}$) around the conductor:

$$\nabla \times \mathbf{B} = \mu \mathbf{j} + \mu\epsilon \partial \mathbf{E}/\partial t \tag{1}$$

In a coaxial cable, this inductance is usually compensated by the inductance of return currents flowing through the shielding. The magnetic inductances annul each other outside of the cable, if the currents on inner and outer conductors are opposed and equal in magnitude. In the probe setup of Fig. 1, the currents flow from the power supply through the Langmuir-Hotlink device and the inner conductor of the probe cables to the probe tips, into the plasma, parallel to the magnetic field lines into the divertor and from the divertor through the separate ground connection back to the power supply. The current does not flow through the shielding of the coaxial cables. The magnetic inductance of probe currents does not cancel in this case and can influence neighboring cables. When the current through one probe varies, the magnetic inductance between outer and inner conductor of the neighboring coaxial cable varies as well. This magnetic inductance can induce an electric field according to Faraday's law:

$$\partial \mathbf{B}/\partial t = -\nabla \times \mathbf{E} \tag{2}$$

In the plane perpendicular to the circular magnetic field, the coaxial cable can be approximated by two conductor loops (Fig. 11a). One loop consists of the closer shielding and the inner conductor while the other loop consists of the inner conductor and the shielding further away from the source current. Both loops are connected with each other at the inner conductor and via the shielding. The induced electric fields annul each other if the magnetic inductance is identical in both loops. $\mathbf{B}$ of a current filament decreases like $1/r$ with the distance r from the current filament. Therefore, the voltages induced on both sides of the coaxial cable do not cancel out and lead to an induced net voltage. The voltages induced in each conductor loop are given by the integral around one half of the coaxial cross section with length $l \approx 10\,\mathrm{m}$ and width $r_2 - r_1 \approx 1\,\mathrm{mm}$:

$$U_{\mathrm{ind}} = \oint \mathbf{E} d\mathbf{s} = -\oint \frac{\partial \mathbf{B}}{\partial t} d\mathbf{A} \tag{3}$$

$$= -\oint \frac{\mu}{2\pi r} \frac{\partial \mathbf{I}}{\partial t} d\mathbf{A} = -\frac{\mu l}{2\pi} \frac{\partial I}{\partial t} \ln(r_2/r_1).$$

The net voltage U_{tot} induced in the coaxial cable is given by the difference of the voltages induced on both sides of the inner conductor:

$$U_{\mathrm{tot}} = U_{\mathrm{ind,a}} - U_{\mathrm{ind,b}} = -\frac{\mu_0 \mu_{\mathrm{r}} l}{2\Pi} \frac{\partial I}{\partial t} \ln(\frac{r_{2a}\ r_{1b}}{r_{1a}\ r_{2b}})$$

$$= -2 \times 10^{-7}\,\frac{\mathrm{H}}{\mathrm{m}}\ 10\,\mathrm{m}\ 1.3 \times 10^{6}\,\frac{\mathrm{A}}{\mathrm{s}}\ \ln(\frac{4.7\,\mathrm{mm}\ 5.7\,\mathrm{mm}}{3.7\,\mathrm{mm}\ 6.7\,\mathrm{mm}}) \approx -0.2\,\mathrm{V} \tag{4}$$

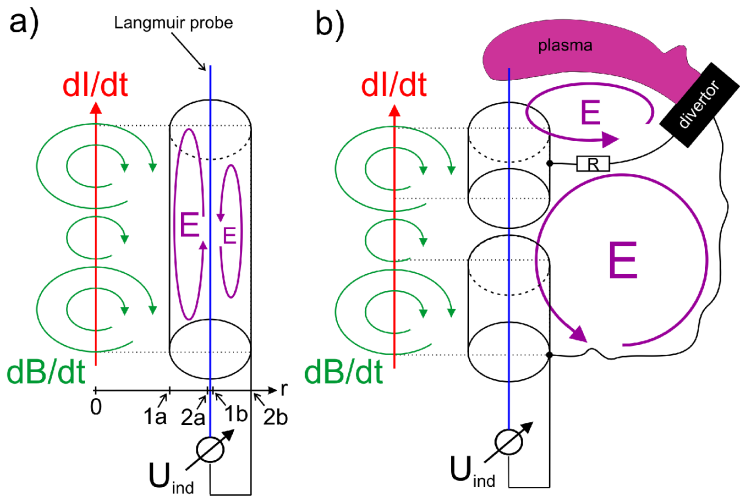

Figure 11: Inductance in coaxial cables driven by the current modulation in an unshielded parallel cable. a) Simple coaxial cable. b) Interrupted shielding with separate ground connection from plasma to measurement.

This corresponds to a coupling inductance of $L_{\text{cables}} \approx 0.16\,\mu\text{H}$ between two close parallel coaxial cables of 10 m length and missing return currents. This result is more than two orders of magnitude below the coupling inductance $L_{\text{exp}} \approx 80\,\mu\text{H}$ found experimentally in the previous subsection.

However, the shielding of the coaxial cables was interrupted in the manipulator setup, as shown in Figs. 11b) and Fig. 1. One part is grounded at the vacuum feed-throughs on the midplane and the diagnostic part is grounded separately at the divertor. A better approximation of the coupling inductance can be obtained by integrating over the whole surface defined by inner conductor, ground connection, divertor and plasma or vacuum vessel. Assuming a distance of 1 cm between the inner conductors of the cables and 5 m between cable and ground connection leads to the coupling inductance $L_{\text{approx}} \approx 6\,\mu\text{H}$. The small contribution of the coaxial cable itself is neglected. This result has been confirmed experimentally in laboratory measurements as shown in the next subsection, but it is still one order of magnitude below the strong coupling inductance observed in the torus hall.

4.3 Laboratory evidence

Laboratory experiments have been performed to verify the theoretical considerations from the previous subsection. Three different setups have been tested in the laboratory to model the cross-talk of probes on the midplane manipulator of ASDEX Upgrade. Setup A consisted of two coaxial cables with interrupted outer conductors (Fig. 1). In setup B, the outer conductors were connected across the gap with unshielded cables and the external ground connection was

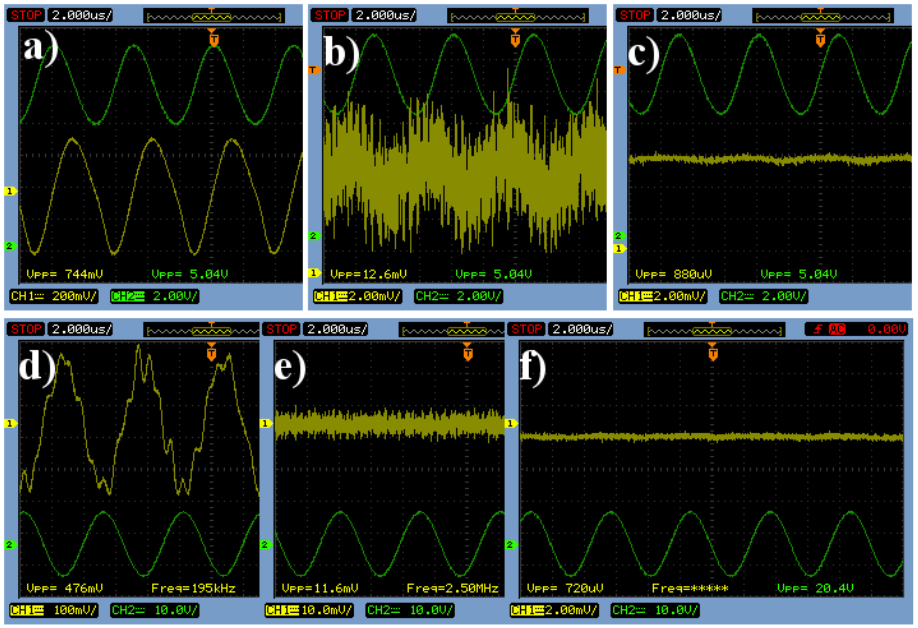

Figure 12: Inductive (top) and capacitive coupling (bottom) for different connection setups: interrupted shielding (a, d), connected shieldings (b, e) and continuous shielding (c, f). The excitation signal (green) is the same, but the cross-talk amplitude on a free-floating probe channel (yellow) changes with the connection setup.

interrupted to avoid a ground loop. Setup C consisted of continuously shielded coaxial cables (Fig. 2). The response of these setups has been checked for current and voltage modulation to separate inductive and capacitive coupling mechanisms.

In real plasma experiments, ion-saturation current measurements are for example modulated when high density events like blobs or ELMs pass the probe. In the laboratory, such a changing plasma impedance was simulated with a transistor instead of the probe head. A constant bias voltage of 15 V has been applied on the opposite side of the cable. The current through this cable has been modulated by a ground free control current through the transistor. An average current of more than 100 mA was flowing through the cable with a peak to peak modulation of 50 mA at 200 kHz. This modulation amplitude and frequency correspond to what is also observed in plasma experiments. The top row of Figure 12 shows the results of this inductive coupling analysis. The upper curves (green) indicate the current modulation with $5\,\mathrm{V_{pp}}$, corresponding to $50\,\mathrm{mA_{pp}}$. The cross-talk amplitude (yellow) is measured on a parallel cable with the same connection setup as the current modulated line. This corresponds to a neighboring floating potential measurement in absence of plasma. Setup A reveals a

cross-talk amplitude $U_{\mathrm{pp}} \approx 750\,\mathrm{mV_{pp}}$ (Fig. 12a). Variations of the unshielded cable length or position do not change the cross-talk amplitude significantly. Even overlapping, but still interrupted shields do not decrease this cross-talk amplitude. The amplitude decreases by two orders of magnitude, when the cable shields are connected in setup B (Fig. 12b) and by another order for continuous coaxial cables in setup C (Fig. 12c). This confirms the cancellation of inductive cross-talk between continuous coaxial cables. The coupling inductances deduced from this experiment are $L_{\mathrm{lab}} = U_{\mathrm{pp}}/2 \times (dI/dt)^{-1} \approx 20$, 0.3 and $< 0.02\,\mu\mathrm{H}$, respectively for the setups A, B and C. The coupling inductance of setup A is in the range of what was expected in the previous subsection ($6\,\mu\mathrm{H}$). For the continuously shielded cables of setup C, the coupling inductance is below the expected value of $0.2\,\mu\mathrm{H}$. This might be explained by the larger distance of the cables in the lab, than in the theoretical model. The laboratory experiments agree qualitatively with the theoretical predictions and show that the inductive cross-talk of Langmuir probes was indeed related to the interrupted shieldings at the end of the manipulator.

Furthermore, probe signals can cross-talk due to potential variations. In real experiments, the probe potentials can vary because of plasma fluctuations or swept bias voltages. The lower row in Figure 12 shows the simulation results of such potential cross-talk for the cable setups A, B and C. A sinusoidal wave was applied to one cable (lower curve, green) and the response of a neighboring cable was measured (upper curve, yellow). Open ends of the cables represented the Langmuir probe head in absence of plasma. One cable was excited with 200 kHz and $20\,\mathrm{V_{pp}}$. A cross-talk amplitude of almost $500\,\mathrm{mV_{pp}}$ was observed for setup A (Fig. 12d). No cross-talk was observed for setup B and C (Fig. 12e and f). This capacitive cross-talk can be explained with the capacitance of the front part of the cables in setup A (Fig. 1). Currents flow through the bellows resistance to charge and discharge the front capacitance of the excited cable with the applied bias voltage. The currents cause a potential difference at the resistance, which is transmitted capacitively to the inner conductor of the other cables and measured as cross-talk signal. This finding supports the need of a continuous shielding and one single grounding point for Langmuir probe experiments. Inductive and capacitive coupling between neighboring probe channels are eliminated if only one single connection point is present between the two circuits, as shown in Fig. 2.

4.4 Suppression at AUG

The laboratory tests presented in the previous subsection have been confirmed by measurements with the original equipment and connections, to eliminate remaining doubts. At first, the cables in the manipulator arm were tested without vessel and additional cables. Currents of $50\,\mathrm{mA_{pp}}$ at 200 kHz caused potential perturbations $< 1\,\mathrm{mV}$ on neighboring channels. The application of $20\,\mathrm{V_{pp}}$ at 200 kHz caused no cross-talk at all. The cables inside the manipulator are continuously shielded.

The final prove was obtained with the manipulator on location in the torus

hall, to assure correct ground connections and the use of the same cables as in real experiments. A probe head was not mounted on the manipulator, to show that the cross-talk is independent of the probe head. Two manipulator channels were connected inside the vacuum vessel. The current through this loop was modulated again with the previously mentioned ground free transistor circuit. The current path went from the power supply to Langmuir-Hotlink device, along the inner connector of the probe cables into the vaccum vessel and back throut the second connected wire. At the manipulator exit, it was modulated and connected with a cable to the divertor, as it would be the case in presence of plasma. This setup enabled a realistic modulation of the probe currents in the manipulator without entering the vacuum vessel. The capacitive coupling was investigated on two neighboring manipulator channels with open endings inside the vacuum vessel. Figure 13 shows the inductive (top) and capacitive (bottom) coupling between independent manipulator channels in the torus hall of ASDEX Upgrade with the cabling setup A, as it was used routinely before the experimental campaign in 2010 (left side), and with the cabling setup B, as it is used since autumn 2010 (right). Both, inductive and capacitive cross-talk are reduced by at least tree orders of magnitude. This confirms the model developed in the previous subsections and provides for more reliable measurements. In the new setup, the shieldings are connected in the metal box at the end of the manipulator and grounded only at the vacuum feed-throughs.

The coupling inductance of the manipulator deduced from Fig. 13a is about $170\,\mu$H. This is in the same range as the $80\,\mu$H obtained from experimental data analysis in Sec. 3. A finite resistance of $1.5\,\Omega$ was measured along the ground connection, that is probably linked to the manipulator bellows (see Fig. 1). This resistance leads in presence of the 50 mApp current modulation to a $75\,\mathrm{mV_{pp}}$ variation of manipulator potential. This manipulator potential acts as reference potential for all measurements on the manipulator, as they are in direct contact at the vacuum feed-throughs. This modulation amplitude is much lower than the 1.66 Vpp for inductive coupling due to the interrupted shieldings in Fig. 13a). However, it has to be pointed out, that this effect will influence potential measurements, as long as significant currents are drawn over the belows. This problem could be avoided in future with a bypass of the bellows to minimize the resistance of the common ground connection between divertor and manipulator. High probe currents should be avoided, even with a bypass of the bellows in place, because a second inductance loop is still in place (Fig. 11b). It consists of probe tip, plasma, divertor, vacuum vessel and feed-through. Therefore, strong megnetic inductance should always be avoided by limiting the following fast externally driven current changes in future experiments: (i) The abrupt current change at the voltage peak of a triangular swept Langmuir probe can be smoothed with a capacitance parallel to the output of the function generator (lowpass to smooth peaks). (ii) Sweeping probes should not measure up to the electron-saturation current, because otherwise plasma density fluctuations can cause current variations of several hundred k or even MA/s. (iii) The regular interruption of the ion-saturation current bias voltages is not necessary, if power resistors are introduced in series with the probes [13]. The resistors reduce the

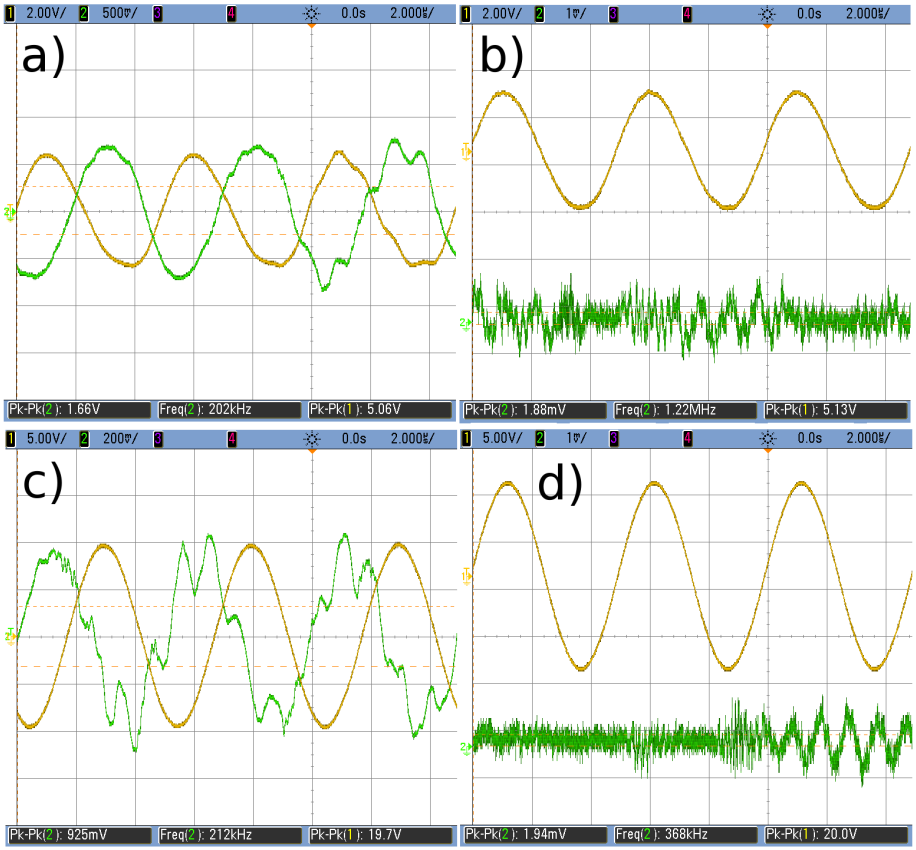

Figure 13: Inductive (top) and capacitive coupling (bottom) with the former manipulator setup (a, c) and continuous ground connection (b, d). The modulation signals are shown in yellow and the cross-talk voltages on a free floating channel in green.

probe voltage as soon as arcs lead to high probe currents. This enables an automatic arc suppression and continuous ion-saturation current measurements. However, the used power resistors should be able to withstand the maximum current for several seconds [14]. All these approaches have been successfully implemented in the ASDEX Upgrade experiments of March 2011.

5 Aliasing

The Langmuir-Hotlink devices convert the probe signals from analog to digital. For this conversion, the signals must not contain frequencies above the Nyquist frequency $f_{\mathrm{Ny}} = 0.5 f_{\mathrm{aq}}$, with the data acquisition frequency $f_{\mathrm{aq}} = 2\,\mathrm{MHz}$. The power of frequencies $f > f_{\mathrm{Ny}}$ in the analog signal is folded to $f < f_{\mathrm{Ny}}$ in the

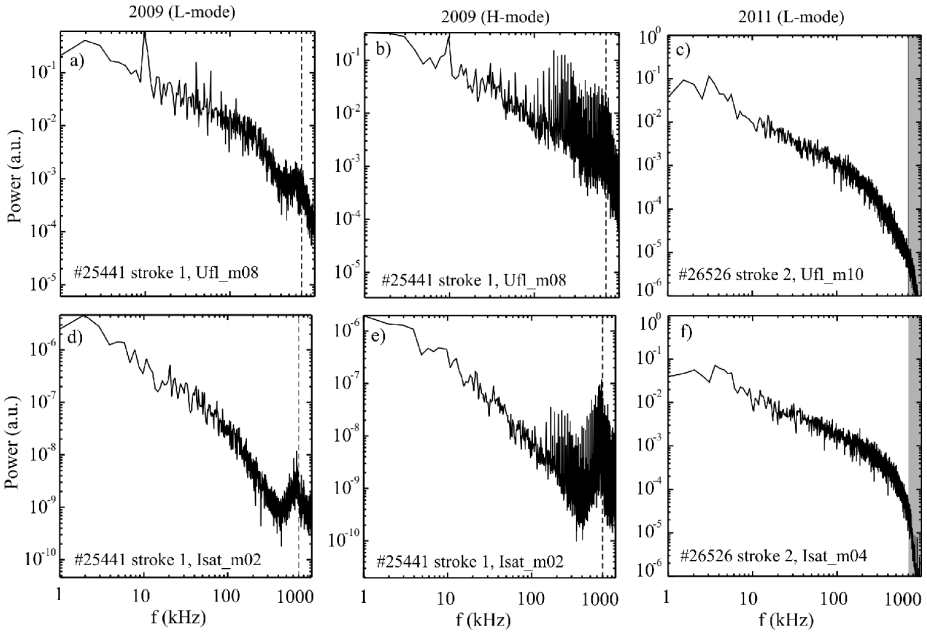

Figure 14: Power spectra of floating potential (top) and ion-saturation current (bottom) during L-mode (left column) and H-mode before circuit modifications (central column) and after (right column). Amplification of high frequency components and aliasing are absent in the right column.

digital signal. It is impossible to remove this aliasing effect from a digitized signal. Aliasing effects are avoided by suppression of high frequencies in the analog signals using low-pass filters with a cut-off frequency below the Nyquist frequency.

Active fourth-order butterworth filters with a cut-off freuquency of 700 kHz were expected to suppress aliasing in the Langmuir-Hotlink devices before March 2011. Butterworth filters are maximally flat in amplitude and linear in phase response [15]. The left and central columns of Fig. 14 show respectively power spectra during L-mode and H-mode phases of a discharge. The digital signals of floating potential (top) and ion-saturation current (below) contain a significant power at frequencies above the cut-off frequency of the anti-aliasing filters (dashed line). The actual output amplitude of the Butterworth filter was measured during a logarithmic frequency scan from 1 k to 50 MHz. As expected, the amplitude is decreasing around the cut-off frequency, but increasing in the MHz range. This behavior of the anti-aliasing filters was found experimentally in the Langmuir-Hotlink devices and confirmed by LTspice simulations. Signals in the MHz range were not suppressed but amplified by the former active filters. Such an amplification can explain the high power at high frequencies in Fig. 14 by aliasing. This unintended behavior was caused by the wrong polarity of the

input signal into the potential-free floating Langmuir-Hotlink devices. Operational amplifiers are not independent of the grounding point of the input signal, because the amplifiers are powered by a positive and a negative DC voltage with respect to ground and not with respect to a fast changing input signal. This behavior of the amplifiers has been reproduced in SPICE simulations and confirmed in laboratory experiments. Before March 2011, the input of the operational amplifier in the Langmuir-Hotlink devices was grounded at the vacuum vessel and its reference potential given by the fluctuating probe signal. This situation is equivalent to the common operational amplifier connection, except for the fluctuation of the reference potential of circuit and power supply. The resonant oscillation of the operational amplifiers vanished after a change of the input polarity. Furthermore, the active filters have been replaced by passive 6th order Chebychev filters with a cut-off frequency of about 800 kHz. The right column of Figure 14 shows floating potential (top) and ion-saturation current (bottom) spectra of Langmuir probe measurements in the ASDEX Upgrade tokamak with passive filters and changed polarity in the improved Langmuir-Hotlink devices. Fluctuations above the cut-off frequency of the anti-aliasing filter are now clearly suppressed. However, some irregularities have been observed in the fluctuating signals of a few Langmuir-Hotlink channels during the experimental campaign in March 2011. Therefore, the frequency response of each channel needs to be rechecked and possibly adapted, to obtain a reliable and comparable probe system on the midplane manipulator of ASDEX Upgrade.

6 Signal transmission

This section investigates the transmission of probe signals from the measurement position inside the vacuum vessel to the Langmuir-Hotlink devices outside. The connecting cable has a finite capacitance and is terminated by a resistance. Such a parallel circuit of a capacitance (C) and resistance (R) represents a first-order low-pass filter with the cut-off frequency

$$f_{\mathrm{cut-off}} = \frac{1}{2\pi RC}. \tag{5}$$

The capacitance of a 20 m long coaxial cable is about 2 nF. For potential measurements, the measurement resistance in the Langmuir-Hotlink device is 1.1 MΩ. On the plasma side, the cable is terminated by the differential plasma impedance at the floating potential. This impedance changes with the plasma conditions at the probe. It varies for free standing cylindrical probes (diameter 1 mm, length 2 mm) from the separatrix to the far SOL from about 50 to 500 Ω. The corresponding cut-off frequencies are given in Table 1. The time constant of the filter is set mainly by the smallest termination resistance, i.e. by the plasma impedance. A larger probe surface in contact with the plasma will further reduce this impedance. In contrary, the limited plasma contact of Ball Pen Probes (BPP) [16] leads to an increased impedance from 500 Ω about 1 cm outside the separatrix to 30 kΩ in a distance of 3 cm [17]. This effect can explain differences between the power spectra of Langmuir probes and BPPs.

coaxial cable		cut-off frequency $f(R, C)$ of cable transmission	
probe setup	with R	without preamplifier $L_{\text{cable}} \approx 20\,\text{m}$ $C \approx 2\,\text{nF}$	with preamplifier $L_{\text{cable}} \approx 5\,\text{m}$ $C \approx 0.5\,\text{nF}$
I_{sat} and U_{sat} (power supply)	$50\,\Omega$	**1.6 MHz**	-
U_{fl} (near SOL)	$50\,\Omega$	1.6 MHz	**6.4 MHz**
U_{fl} (far SOL)	$500\,\Omega$	160 kHz	**640 kHz**
U_{BPP} (near SOL)	$600\,\Omega$	130 kHz	**530 kHz**
U_{BPP} (far SOL)	$30\,\text{k}\Omega$	2.7 kHz	**11 kHz**

Table 1: Cut-off frequency of the transmission lines between probe and Langmuir-Hotlink devices with the setup before and after (bold) March 2011. The cut-off frequency depends on probe setup (biased or floating), probe tip (Langmuir or BPP) and plasma conditions (radial position).

In the ion-saturation branch, the plasma impedance is even bigger. However, for current measurements the measurement resistance in series with the internal resistance of the power supply is typically $50\,\Omega$. The low-pass characteristic of the cables is in this case less dependent on the plasma conditions at the probe.

The low-pass characteristic of the transmission lines is not relevant for current measurements because the cut-off frequency is in this case above the Nyquist frequency. In contrary, potential measurements can be significantly affected by the low-pass filtering of the transmission lines, depending on the plasma parameters. The only possibility to improve the high frequency transmission is a reduction of the cable capacitance, because neither plasma impedance nor measurement resistance can be modified in potential measurements. However, the distance between Langmuir-Hotlink devices and probes could not be reduced. Therefore, the potential measurements have been preamplified in March 2011 about 5 m behind the probes at the manipulator exit. The operational amplifier $LM6171$ is able to drive the cables to the Langmuir-Hotlink devices at the required frequencies.

7 Summary and Conclusions

Three perturbing effects on Langmuir probe signals have been identified, explained and eliminated at the ASDEX Upgrade tokamak. Each of these effects has dominated probe signals in some former measurements. The perturbations could be identified, but it is impossible to substract them from measured plasma fluctuations. The first issue was cross-talk by inductive and capacitive coupling between measurement channels on the midplane manipulator. Since the campaign in 2010, this effect is reduced by more than three orders of magnitude by continous coaxial cables with a single grounding point. This modification reduced also the pick-up of magnetic inductance from the torus hall by about the

same amount. Furthermore, inductive coupling should be avoided by limiting fast externally driven current changes in the probes. The second issue was an amplification of high frequencies close to and above the Nyquist frequency by a malfunction of the Langmuir-Hotlink devices. The active anti-aliasing filters caused aliasing of the digitized signals before March 2011. Changing the input polarity and replacing the active Butterworth filters by passive Chebychev filters eliminated this effect. The third issue was the suppression of potential fluctuations above 200 kHz by the transmission lines. The cut-off frequency of the cables was increased in March 2011 with preamplifiers at the exit of the manipulator to more than 600 kHz. The exact frequency depends on the differential plasma impedance at the floating potential and varies with probe geometry and plasma parameters.

Plasma fluctuation measurements with Langmuir probes have been improved on the midplane manipulator and filament probe of ASDEX Upgrade. Previous investigations of radial profiles and low frequency plasma variations might not be affected. However, physics results based on turbulent fluctuations measurements should be reviewed with the new setup, especially if based on potential measurements with the midplane manipulator. Furthermore, it has been shown recently, that floating potential measurements close to the separatrix in ASDEX Upgrade are strongly influenced by electron temperature fluctuations and do not reflect directly the plasma potential fluctuations [18]. Generally, the frequency response and cross-talk amplitude of Langmuir probe systems should be routinely checked before experimental campaigns. This work is intended as a call for precise fluctuation studies and as a guide line to identifiy and suppress probe perturbations.

Acknowledgments

BN thanks V. Rohde, P. Leitenstern and M. Bennewitz, K.-H. Schlüter and F. Müller for support and useful discussions.

References

[1] V. Naulin, J. Nucl. Mater. **363 - 365**, 24 (2007).

[2] J. A. Boedo *et al.*, Phys. Plasmas **8**, 4826 (2001).

[3] G. Antar, M. Tsalas, E. Wolfrum, and V. Rohde, Plasma Phys. Controll. Fusion **50**, 095012 (2008).

[4] B. Nold *et al.*, Plasma Phys. Controll. Fusion **52**, 065005 (2010).

[5] H. W. Müller *et al.*, Nucl. Fusion **51**, 073023 (2011).

[6] A. Schmid *et al.*, Rev. Sci. Instrum. **78**, 053502 (2007).

[7] Schilling, Langmuir-Hotlink, IPP Elektronik E1 (2005).

[8] H. W. Müller, Welcome to the LangmuirProbes web (1st August 2012) *https://www.aug.ipp.mpg.de/augtwiki/bin/view/LangmuirProbes/WebHome*.

[9] L. Kammerloher, Langmuir-Hotlink, IPP Elektronik E1 (2010).

[10] H. W. Müller *et al.*, Contrib. Plasma Phys. **50**, 847 (2010).

[11] M. Weinlich and A. Carlson, Phys. Plasmas **4**, 2151 (1997).

[12] H. Stöcker, *Taschenbuch der Physik* (Harry Deutsch, Frankfurt a. M., 2007).

[13] J. Bleuel, IPP-Report III/235.

[14] H. W. Müller, private communication (2011).

[15] S. Butterworth, The Wireless Engineer **7**, 536 (1930).

[16] J. Adamek *et al.*, J. Nucl. Mater. **390-391**, 1114 (2009).

[17] J. Horacek, private communication (2010).

[18] B. Nold *et al.*, New J. Phys. **14**, 063022 (2012).